

Accepted Manuscript

Synthesis of C₅-tethered indolyl-3-glyoxylamide derivatives as tubulin polymerization inhibitors

Sravanthi Devi Guggilapu, Guntuku Lalita, T. Srinivasa Reddy, Santosh Kumar Prajapati, Atulya Nagarsenkar, Shymala Ramu, Uma Rani Brahma, Uppa Jaya Lakshmi, Ganga Modi Naidu Vegi, Suresh K. Bhargava, Bathini Nagendra Babu

PII: S0223-5234(17)30035-1

DOI: [10.1016/j.ejmech.2017.01.026](https://doi.org/10.1016/j.ejmech.2017.01.026)

Reference: EJMECH 9177

To appear in: *European Journal of Medicinal Chemistry*

Received Date: 4 November 2016

Revised Date: 19 January 2017

Accepted Date: 19 January 2017

Please cite this article as: S.D. Guggilapu, G. Lalita, T.S. Reddy, S.K. Prajapati, A. Nagarsenkar, S. Ramu, U.R. Brahma, U.J. Lakshmi, G.M.N. Vegi, S.K. Bhargava, B.N. Babu, Synthesis of C₅-tethered indolyl-3-glyoxylamide derivatives as tubulin polymerization inhibitors, *European Journal of Medicinal Chemistry* (2017), doi: 10.1016/j.ejmech.2017.01.026.

This is a PDF file of an unedited manuscript that has been accepted for publication. As a service to our customers we are providing this early version of the manuscript. The manuscript will undergo copyediting, typesetting, and review of the resulting proof before it is published in its final form. Please note that during the production process errors may be discovered which could affect the content, and all legal disclaimers that apply to the journal pertain.



Synthesis of C₅-tethered Indolyl-3-glyoxylamide derivatives as Tubulin Polymerization

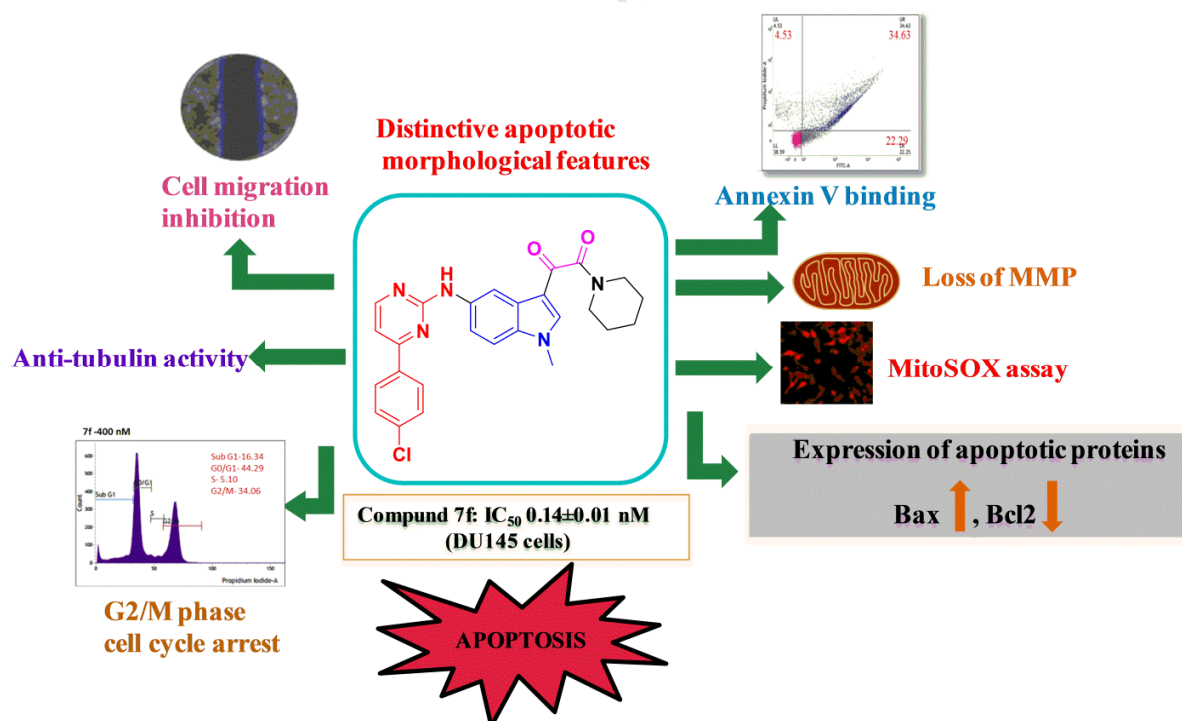
Inhibitors

Sravanthi Devi Guggilapu,^a Guntuku Lalita,^b T. Srinivasa Reddy,^c Santosh Kumar Prajapati,^a Atulya Nagarsenkar,^a Shymala Ramu,^a Uma Rani Brahma,^b Uppa Jaya Lakshmi,^b Ganga Modi Naidu Vegi,^b Suresh K. Bhargava,^c and Bathini Nagendra Babu^{a*}

^aDepartment of Medicinal Chemistry, National Institute of Pharmaceutical Education and Research (NIPER), Hyderabad 500 037, India

^bPharmacology and Toxicology Division, National Institute of Pharmaceutical Education and Research (NIPER), Hyderabad 500 037, India

^cCentre for Advanced Materials & Industrial Chemistry (CAMIC), School of Science, RMIT University, GPO BOX 2476, Melbourne-3001, Australia.



Synthesis of C₅-tethered Indolyl-3-glyoxylamide derivatives as Tubulin Polymerization**Inhibitors**

Sravanthi Devi Guggilapu,^a Guntuku Lalita,^b T. Srinivasa Reddy,^c Santosh Kumar Prajapati,^a
Atulya Nagarsenkar,^a Shymala Ramu,^a Uma Rani Brahma,^b Uppa Jaya Lakshmi,^b Ganga
Modi Naidu Vegi,^b Suresh K. Bhargava,^c and Bathini Nagendra Babu^{a*}

^a*Department of Medicinal Chemistry, National Institute of Pharmaceutical Education and Research (NIPER), Hyderabad 500 037, India*

^b*Pharmacology and Toxicology Division, National Institute of Pharmaceutical Education and Research (NIPER), Hyderabad 500 037, India*

^c*Centre for Advanced Materials & Industrial Chemistry (CAMIC), School of Science, RMIT University, GPO BOX 2476, Melbourne-3001, Australia.*

*Corresponding author:

Dr. Bathini Nagendra Babu

Department of Medicinal Chemistry

National Institute of Pharmaceutical Education and Research

Hyderabad, 500037, India

E-mail: bathini@niperhyd.ac.in; bnniper@gmail.com

Abstract

A series of C₅-tethered Indolyl-3-glyoxylamide derivatives were synthesized and evaluated for their *in vitro* cytotoxic activity against DU145 (prostate), PC-3 (prostate), A549 (lung) and HCT-15 (colon) cancer cell lines by employing the 3-(4,5-dimethylthiazol-2-yl)-2,5-diphenyltetrazolium bromide (MTT) assay. Among all the synthesized compounds, compound **7f** displayed cytotoxicity of IC₅₀ = 140 nM towards DU145 cancer cell line. The treatment of DU145 cells with **7f** led to inhibition of cell migration ability. Further, the detailed studies such as acridine orange/ethidium Bromide (AO/EB), DAPI, annexin V-FITC/propidium iodide staining assay suggested that the compound **7f** induced apoptosis in DU145 cells. The influence of the cytotoxic compound **7f** on the cell cycle distribution was assessed on the DU145 cell line, exhibiting a cell cycle arrest at the G2/M phase (hallmark of tubulin polymerization) and next inhibited tubulin polymerization with IC₅₀ 0.40 μM. Furthermore, the treatment with compound **7f** caused collapse of mitochondrial membrane potential and elevated intracellular superoxide ROS levels in DU145 cells. Western blotting was performed to examine the levels of apoptotic proteins (Bcl-2 and Bax); the study confirmed that compound **7f** induced apoptosis through apoptosis-related protein expression. Thus, these studies provided a new molecular scaffold for the further development of anticancer agents that target tubulin.

Keywords: indolyl-3-glyoxylamide, anticancer, apoptosis, tubulin polymerization inhibitor.

1.0 Introduction

Cancer is one of the foremost global health burden and severe clinical problems in the world with increasing frequency every year. Hormones, immune conditions, inherited genes, viruses, chemicals and radiation are some of the responsible factors for the development of various cancers [1]. The uncontrolled growth and spreading of abnormal cells results in the disruption of tissues that leads to death in cancer patients [2, 3]. Many of the currently available antitumor drugs are unable to differentiate between normal and neoplastic cells or to overcome primary or secondary resistance mechanisms evolved in the tumor cells. The high toxicity and poor tolerance of the existing anticancer drugs, stress on the need to identify novel molecules with potent antitumor activity, low toxicity and minimum side effects.

Recent drug discovery studies have focused on the design and synthesis of small molecules that have an indole nucleus as the core structure and that act as tubulin inhibitors [4]. Tubulin polymerization inhibitors interfere with the dynamic instability of microtubules, causing disruption of microtubules, and thereby inducing cell cycle arrest in the M-phase, resulting in the apoptotic cell death [5]. Anti-mitotic compounds such as taxanes and vinca alkaloids have been widely used in the clinical treatment of different human cancers over the past decade [6]. Unfortunately, clinical use of these compounds are restricted by toxicity, drug resistance, and limited bioavailability [7, 8]. This has encouraged medicinal chemists to design and synthesize novel anti-mitotic agents for cancer therapy.

The indole ring system is an essential part of several tubulin inhibitors identified in the recent years including the indolyl-3-glyoxamide, Indibulin and the 2-arylindoles, D-64131 (**Figure 1**). *N*-(pyridin-4-yl)-[1-(4-chlorobenzyl)-indol-3-yl]-glyoxyl-amide (Indibulin) is a novel synthetic compound that was identified in a cell-based screening

assay to discover cytotoxic drugs. Indibulin destabilizes microtubules via a direct interaction with tubulin at a binding site, distinct from those of the known destabilizing tubulin agents vincristine or colchicines [9]. Indibulin blocks cell cycle transition specifically at G2/M-phase and leads to subsequent cell death [10].

On the other hand, aminopyrimidines, an important pharmacophore present in many anticancer drugs, are also found as tubulin polymerization inhibitors. Aminopyrimidines (**Figure 1**) have been identified to possess potent antitumour and tubulin depolymerization activity [11, 12]. More interestingly, Hu *et al.* documented that compound (**e**), generated by introduction of indole moiety into pyrimidine (**d**) displayed threefold improvement in inhibiting tubulin polymerization compared to compound (**d**) [13]. Moreover, some of the naturally occurring the indolyl-pyrimidines [14, 15] such as meridianin, hyrtinadine, and aplicyanin are also reported for their anticancer potentials (**Figure 1**) [16, 17].

<Insert Figure 1 here>

Therefore, owing to our interest in the synthesis of biologically active scaffolds [18], we envisioned to synthesize indolyl-3-glyoxylamide derivatives with an array of substitutions, which may lead us towards an enhancement in cytotoxic activity. In order to develop pertinent leads for prospective tubulin inhibitors, we have introduced appropriate substitutions at C-5 positions of indolyl-3-glyoxylamide derivatives by performing Ullmann type C-N bond coupling reaction or constituting C-C bond *via* Suzuki coupling reaction.

<Insert Figure 2 here>

2.0 Results and discussion

2.1 Chemistry

The synthetic protocol to achieve target molecule involved five steps (**Scheme 1**), which incites from synthesis of different substituted aromatic and heteroaromatic enamines **2(a-i)** by employing respective acetophenones **1(a-i)** and refluxing it with DMF–DMA to obtain desired products in quantitative yields [19]. During the course of product formation, methanol was formed as a by-product which was distilled off at regular intervals, as it can intervene with the proceedings of reaction. The synthesized enaminone intermediates **2(a-i)** were further subjected to reflux with guanidine nitrate in *n*-butanol under basic condition to afford respective aminopyrimidines **3(a-i)** in high yields [20]. On the other hand, the indolyl-3-glyoxylamides were prepared by treatment of 5-bromo indole (**4**) with oxalyl chloride at 0 °C in diethyl ether produced the 2-(5-bromo-1*H*-indol-3-yl)-2-oxoacetyl chloride due to the high nucleophilic character at 3-position of indole and followed by substitution reaction with piperidine in presence of mild base triethylamine afforded compound (**5**) in 87% yield [21]. This was succeeded by *N*-methylation to acquire 1-(5-bromo-1*H*-indol-3-yl)-2-(piperidin-1-yl)ethane-1,2-dione (**6**), in high yields.

Finally, the two privileged moieties **3(a-i)** and **6** were subsequently linked through Ullmann type C–N bond coupling reaction to yield compounds **7(a-i)** [22]. In this reaction, CuI was utilized to carry out the coupling under strict anhydrous atmosphere, as the presence of moisture impeded the progress of reaction. As aminopyrimidines are very weak nucleophiles, a strong electron donating agent such as DMEDA was added under the basic condition of Cs₂CO₃, to carry out the reaction. Additionally, the substrate (**6**) was subjected to Suzuki coupling reaction with the relevant boronic acids and palladium catalyst tetrakis(triphenylphosphine) palladium (0), to afford the compounds **8(a-f)** [23]. All the

synthesized compounds **7a–7i** and **8a–8f** were confirmed by using FT-IR, ¹H NMR, ¹³C NMR and HRMS (ESI) spectroscopic techniques.

<Insert Scheme 1 here>

2.2 Pharmacology

2.2.1. *In vitro* anticancer activity

All the newly synthesized compounds were evaluated for their *in vitro* cytotoxic activity against DU145, PC-3, A549 and HCT-15 cancer cell lines by employing the 3-(4,5-dimethylthiazol-2-yl) -2,5-diphenyltetrazolium bromide (MTT) assay [24]. Indibulin and podophyllotoxin were used as reference for this study. The concentration response course analysis was performed to determine drug concentrations required to inhibit the growth of cancer cells by 50% (IC₅₀) after incubation for 48 h. The results from the *in vitro* anticancer studies exposed that the synthesized target compounds exhibited different levels of anticancer properties (Table 1). From the close examination of the IC₅₀ values, it was observed that, pyrimidine linked indolyl-3-glyoxylamide with phenyl substitution (**7a**) was inactive against all tested cancer cell lines while the phenyl substituted with electron donating groups such as –Me (**7b**) and –OMe (**7c**) at *para* position did not offer much improvement in activity, except that the compound **7c** was specifically active against HCT-15. When the phenyl ring is introduced with free hydroxyl group at *para* position (**7d**), the compound was inactive against all the tested cancer cell lines. Interestingly, introduction of electron withdrawing groups at *para* position of phenyl ring such as –F (**7e**), –Cl (**7f**) displayed enhanced inhibitory activity against all the tested cancer cell lines. The compound **7f** displayed excellent inhibitory activity. Notably, the cytotoxicity decreased while

substituting the phenyl ring with groups such as *p*-CF₃ (**7g**). Moreover, the replacement of phenyl group with the heterocyclic substituents such as pyridine (**7h**) and thiophene (**7i**), displayed moderate activity however; the compound **7h** was specifically active against A-549.

On the other hand, the series of compounds **8a-8f** bearing aromatic ring at 5th position displayed no significant activity although the compound **8b**, having –Me group at *para* position of phenyl ring evidenced moderate activity towards HCT-15.

Analysis of the MTT assay results suggests that DU145 cells are more sensitive towards the synthesized target compounds. The impact of modification of the “R” group in series (**7a-7i**) is interesting in the light of the results of the SAR study, which suggests that presence of electron withdrawing groups such as –F (**7e**) and –Cl (**7f**) is optimal for anticancer activity. On the other hand simple substitutions at 5th position such as in the series (**8a-8f**) demonstrated decrease in the activity. This represents that bulky substitution such as 4-aryl pyrimidine moieties (**7a-7i**) should be present at 5th position for improvement in anticancer potential. Among all compounds synthesized, compound **7f** showed the most significant cytotoxicity towards all the tested cancer cell lines. These primary results persuade further investigation on the synthesized compounds aiming to the development of novel potential anticancer agents to target tubulin.

<Insert Table 1 here>

2.2.2. Wound healing assay

Wound healing assay was carried out to investigate the effect of compound **7f** on migration potential of DU145 cells [25]. The number of cells migrated in to the wound area were captured using phase contrast microscope after 0, 12 and 24 h incubation. The results from the **Figure 3** clearly showed that wound gap in control has decreased considerably by

migration of cells in control after 24 h, whereas the treatment with 100, 200 and 400 nM of compound **7f** significantly inhibited the migration of cells in to the scratch area by 61.6%, 52.1% and 47.2% respectively. It can be inferred from the results that the compound **7f** suppresses the migration potential of the DU145 cells in dose dependent manner.

<Insert Figure 3 here>

2.2.3. Acridine orange–ethidium bromide (AO–EB) staining

Acridine orange/ethidium bromide (AO/EB) fluorescent staining assay was performed to differentiate the live, apoptotic and necrotic cells [26]. AO permeates the intact cell membrane and stains the nuclei green, while EB can stain the cells that have lost their membrane integrity and tinge the nucleus red. It can be interpreted from **Figure 4** that the control cells showed the normal morphology and appeared green in colour. Fluorescence microscopic images of **7f** treated DU145 cells have clearly demonstrated morphological changes which are the characteristic features of apoptotic cells such as cell membrane blebbing, chromatin condensation, destructive fragmentation of chromatin, cell shrinkage and apoptotic body formation. This confirms that the compound **7f** induced cell death in DU145 cancer cells.

<Insert Figure 4 here>

2.2.4 DAPI Nucleic Acid Staining

DAPI (4',6-diamidino-2-phenylindole) is a fluorescent dye that binds firmly to nucleus and detect the nuclear damage or chromatin condensation. The DAPI stains the apoptotic cells by forming bright colored fluorescent complexes with chromatin, which is a unique apoptotic feature. Therefore, it was of our interest to detect nuclear

damage or chromatin condensation induced by the compound **7f** in DU145 cells. DAPI staining technique was performed according to an earlier reported method [27]. The results from the **Figure 5** revealed that the nuclear structure of control cells was intact whereas compound **7f** treated cells exhibited horse shaped or fragmented nuclei.

<Insert Figure 5 here>

2.2.5 Cell cycle analysis

Many of the cytotoxic compounds exert their growth inhibitory effect by arresting the cell cycle at a specific phase of a cell cycle. *In vitro* screening results revealed that the compound **7f** showed significant activity against DU145 cells. Thus, we herein examined the effect of the compound **7f** on cell cycle using propidium iodide staining method [28]. DU145 cells were treated with increasing concentrations of compound **7f** for 24 h. They were stained with propidium iodide and samples were further analysed by flow cytometry. Treatment with the compound **7f** at 200 and 400 nM in DU145 cells displayed rise in G2/M population from 24.71% (control) to 28.65% and 34.06% respectively in a dose dependent manner (**Figure 6**). In case of podophyllotoxin (standard), the ratio of cells in G2/M phase increased from 24.71% in control to 61.48% at 400 nM. These results indicate G2/M cell cycle arrest by the test compound suggesting the induction of apoptotic death in the treated cells.

<Insert Figure 6 here>

2.2.6 Annexin V binding assay

To quantify the percentage of apoptosis induced by compound **7f**, the annexin V-FITC/propidium iodide staining assay was carried out using prostate DU145 cancer cells [28]. DU145 cells were treated with 200 nM and 400 nM of compound **7f** for 24

h and stained with Annexin V-FITC and propidium iodide, and samples were analysed by flow cytometry.

As depicted in **Figure 7**, **7f** treated DU145 cells demonstrated rise in the total percentage of apoptotic (early and late apoptotic cells- Annexin V +ve cells) and dead cells from 4.11% (control) to 14.22% (200 nM), 61.45% (400 nM) respectively in a dose dependent manner while the standard indibulin displayed 49.68% of apoptotic (early and late apoptotic cells- Annexin V +ve cells) and dead cells at 400 nM.

<Insert Figure 7 here>

2.2.7 Analysis of Mitochondrial Membrane Potential ($D\Psi_m$)

Mitochondria play a key role in energy metabolism, as they build their membrane potential from respiratory substrates derived from the electron transport chain. Literature reports indicate that the loss or collapse of mitochondrial membrane potential may be an early event in the process of apoptosis [29]. Thus, the effect of compound **7f** on mitochondrial membrane potential ($D\Psi_m$) was determined by staining with lipophilic cationic JC-1 dye [30]. Healthy polarised mitochondria stains red due to potential dependent formation of J-aggregates, while depolarised mitochondria in apoptotic cells stains green because of J-monomers. DU145 cells were treated with 200 nM and 400 nM of **7f** for 24 h and stained by JC-1 dye. Flow cytometric analysis of the treated cells clearly displayed increase in depolarised cell population (P3) from control (19.06%) to 32.55% and 35.92% respectively and with 400 nM of podophyllotoxin the depolarised cell population (P3) increased from control (19.06%) to 36.35% (**Figure 8**). Thus, the results clearly indicate loss of mitochondrial membrane potential by the compound **7f** and suggest the involvement of mitochondria dependent apoptotic pathway in their mechanism of action.

<Insert Figure 8 here>

2.2.8 Measurement of superoxide levels (MitoSOXTM red assay)

The production of ROS has been implicated in apoptotic induction by triggering oxidative damage to the mitochondrial membrane potential and permeability [31]. We were intrigued by the fact that the apoptosis induction could be due to the ROS generation. Henceforth, we tested this possibility using MitoSOXTM red; a chemical probe which reacts with mitochondrial generated superoxide and accumulates in mitochondria [32]. MitoSOXTM Red is a novel fluorogenic dye which selectively detects superoxide in the mitochondria of live cells. MitoSOXTM red is quickly oxidized by superoxide species but not by other reactive oxygen species (ROS) and reactive nitrogen species (RNS). The oxidized product is highly fluorescent upon binding to nucleic acid and produces red fluorescence. Fluorescent microscopic images of DU145 cancer cells stained with MitoSOXTM Red indicator were taken after 48 h treatment with different concentrations of the compound **7f**. It can be easily inferred from the **Figure 9** that the treatment of compound **7f** caused a dose-dependent increase in MitoSOXTM Red fluorescence in DU145 cancer cells. DMSO treated control DU145 cancer cells exhibited weak and diffuse MitoSOXTM Red fluorescence, however the cells treated with 100 nM, 200 nM and 400 nM of compound **7f** were brightly stained suggesting superoxide generation.

<Insert Figure 9 here>

2.2.9 Effect on tubulin polymerization

The compound **7f** displayed G2/M cell cycle arrest which is a hallmark of tubulin polymerization [33], we investigated the antiproliferative activity of **7f** on ability to

inhibit tubulin polymerization by monitoring the increase in fluorescence emission at 420 nm (excitation wavelength is 360 nm) for 1 h at 37 °C (**Figure 10**). In the assembly assay [34], **7f** and indibulin inhibited 61.4%, 60.5% tubulin polymerization compared to control at 0.5 μ M respectively. While the podophyllotoxin inhibited 77.0% tubulin polymerization compared to control at 5 μ M. The IC₅₀ values of the compound **7f**, indibulin and podophyllotoxin were displayed in **Table 2**.

<Insert Figure 10 here>

<Insert Table 2 here>

2.2.10 Western blotting analysis

Many studies have reported that tubulin polymerization inhibitors induce apoptosis by phosphorylating Bcl-2, reducing the amount of Bcl-2 available to make heterodimers with Bax [35]. Moreover, Bcl-2 family proteins are crucial components of mitochondrial stress-induced cellular apoptosis [36]. Therefore, the expression of apoptosis-related proteins was also determined. Herein, to investigate the molecular mechanisms of compound **7f** on apoptosis, we have checked the expression of Bcl-2 and Bax by using western blot method. Results from the **Figure 11** indicated that compound **7f** down-regulated the expression of anti-apoptotic Bcl-2 and up-regulated the expression of pro-apoptotic Bax proteins in a dose dependent manner, which is a hallmark feature of apoptosis. These protein changes were compared with standard indibulin. Increase in Bax level with compound **7f** was more pronounced than with

standard indibulin treatment. Collectively, these results illustrate that compound **7f** induced apoptosis through apoptosis-related protein expression.

<Insert Figure 11 here>

3.0 Conclusion

In the current study, a series of C₅-tethered Indolyl-3-glyoxylamide derivatives were synthesized, and were further evaluated for their *in vitro* anticancer potentials. An initial screening was performed against human cancer cell lines such as DU145, PC-3, A549 and HCT-15. In MTT assay, the compound **7f** was found to be the most active against DU145 (prostate cancer) cell lines. The treatment of DU145 cells with **7f** led to inhibition of cell migration ability. Further, the detailed studies AO/EB staining, DAPI nuclear staining and Annexin V binding assay suggested that the compound **7f** induced apoptosis in DU145 cells. The cell cycle analysis confirmed G₂/M phase of cell cycle arrest in a dose dependent manner and inhibited tubulin polymerization with IC₅₀ 0.40 μM. Furthermore, depolarization of mitochondrial membrane potential (MMP) was also observed, which indicated that the mitochondrial pathway was also involved in the apoptosis signaling pathway. Moreover, the treatment of **7f** resulted in elevated superoxide ROS levels in DU145 cells. Investigation of expression levels of apoptotic proteins (Bcl-2 and Bax) confirmed that compound **7f** induced apoptosis through apoptosis-related protein expression. The cytotoxicity profile of **7f** in terms of *in vitro* cytotoxicity assay, inhibition of tubulin polymerization and Bcl-2, Bax activation are comparable to the standard indubulin. Thus, it can be concluded that the

C₅-substitution on indolyl-3-glyoxylamide derivatives could also offer potential anti-tubulin leads.

4.0 Experimental protocols

4.1 Chemistry

All reagents and solvents were obtained from commercial suppliers and were used without further purification. Analytical thin layer chromatography (TLC) was performed on MERCK precoated silica gel 60-F-254 (0.5 mm) aluminium plates. Visualization of the spots on TLC plates was achieved UV light. ¹H and ¹³C NMR spectra were recorded on Bruker 500 MHz spectrometers using tetramethyl silane (TMS) as the internal standard. Chemical shifts for ¹H and ¹³C are reported in parts per million (ppm) downfield from tetramethyl silane. Spin multiplicities are described as s (singlet), bs (broad singlet), d (doublet), dd (double doublet), t (triplet), q (quartet), and m (multiplet). Coupling constant (*J*) values are reported in hertz (Hz). IR spectra were recorded on a Perkin Elmer, FT-IR spectrometer using KBr discs. HRMS were determined with Agilent QTOF mass spectrometer 6540 series instrument. Column chromatography was performed using silica gel 60-120.

4.2 General experimental procedure for the synthesis of compounds 7(a-i):

The pyrimidine amine **3a-i** (1.1 mmol), CuI (1.0 mmol) and anhydrous Cs₂CO₃ (2.0 mmol) were added to a round bottom flask along with magnetic stir bar and closed well with a septum. The flask was evacuated and back filled with nitrogen gas three times. Dioxane (15 mL), 1-(5-bromo-1*H*-indol-3-yl)-2-(piperidin-1-yl)ethane-1,2-dione (**6**) (1.0 mmol) and DMEDA (1.0 mmol) were added by syringe at room temperature. The reaction mixture was stirred at 80°C for 20 h under nitrogen atmosphere and then cooled to room temperature. Concentrated ammonia (4 mL) was added, and the mixture was extracted with ethyl acetate

(3X20 mL). The combined organic layer was concentrated *in vacuo*, and the residue was purified by column chromatography on silica gel.

4.3 General experimental procedure for the synthesis of compounds 8(a-f):

1-(5-bromo-1*H*-indol-3-yl)-2-(piperidin-1-yl)ethane-1,2-dione (**6**) (0.48 mmol) was combined with powdered potassium carbonate (200 mg, 1.44 mmol), tetrakis(triphenylphosphine)palladium (0) (3 mg, 0.04 mmol) and the appropriate arylboronic acid (0.52 mmol) in a 25 mL round bottom flask containing toluene (7 mL) and water (3 mL) under nitrogen. The reaction mixture was heated at 80 °C for 6 h with stirring before being cooled, evaporated to dryness under reduced pressure, 10 mL of water was added. Extracted with ethyl acetate (3X10 mL), the ethyl acetate was dried using anhydrous sodium sulfate and evaporated under reduced pressure. The residue was purified by column chromatography on silica gel to obtain the desired compounds **8(a-f)**.

4.3.1 1-(1-methyl-5-((4-phenylpyrimidin-2-yl)amino)-1*H*-indol-3-yl)-2-(piperidin-1-yl)ethane-1,2-dione (7a): White solid; yield: 67%; mp 200-203 °C; IR (KBr): 3292, 2935, 2857, 1615, 1566, 1435, 1411, 1192, 1080, 800, 746 cm⁻¹; ¹H NMR (500 MHz, DMSO-*d*₆) δ 9.73 (1H, s), 9.04 (1H, bs), 8.56 (1H, d, *J* = 5.2 Hz), 8.39 – 8.32 (2H, m), 8.11 (1H, s), 7.60 (1H, dd, *J* = 8.9, 1.8 Hz), 7.57 – 7.51 (4H, m), 7.43 (1H, d, *J* = 5.2 Hz), 3.89 (3H, s), 3.60 (2H, bs), 3.34 (2H, bs), 1.63 (4H, bs), 1.47 (2H, bs); ¹³C NMR (125 MHz, DMSO-*d*₆) δ 185.9, 165.7, 163.2, 160.2, 159.0, 139.9, 136.5, 136.4, 133.1, 130.7, 128.7, 127.0, 125.5, 116.8, 111.8, 110.7, 110.7, 107.2, 46.3, 41.1, 33.2, 25.8, 24.9, 23.8; HRMS: *m/z* calcd for C₂₆H₂₅N₅O₂ [M+H]⁺: 440.2081; found: [M+H]⁺ 440.2089.

4.3.2 1-(1-methyl-5-((4-(*p*-tolyl)pyrimidin-2-yl)amino)-1*H*-indol-3-yl)-2-(piperidin-1-yl)ethane-1,2-dione (7b): White solid; yield: 64%; mp 271-274 °C; IR (KBr): 3340, 2943, 1584, 1581, 1529, 1614, 1445, 1371, 1205, 993, 735 cm⁻¹; ¹H NMR (500 MHz, DMSO-*d*₆) δ 9.69 (1H, s), 9.04 (1H, bs), 8.52 (1H, d, *J* = 5.2 Hz), 8.26 (2H, d, *J* = 7.9 Hz), 8.10 (1H,

s), 7.59 (1H, dd, $J = 8.8, 1.6$ Hz), 7.52 (1H, d, $J = 8.8$ Hz), 7.38 (1H, d, $J = 5.2$ Hz), 7.35 (2H, d, $J = 8.0$ Hz), 3.89 (3H, s), 3.59 (2H, bs), 3.34 (2H, bs), 2.39 (3H, s), 1.63 (4H, bs), 1.48 (2H, s); ^{13}C NMR (125 MHz, DMSO- d_6) δ 185.8, 165.7, 163.2, 160.1, 158.8, 140.6, 139.9, 136.5, 133.7, 133.0, 129.3, 127.0, 125.5, 116.7, 111.8, 110.7, 110.6, 106.9, 46.3, 41.1, 33.3, 25.8, 24.9, 23.8, 20.9; HRMS: m/z calcd for $\text{C}_{27}\text{H}_{27}\text{N}_5\text{O}_2$ $[\text{M}+\text{H}]^+$: 454.2238; found: $[\text{M}+\text{H}]^+$ 454.2234.

4.3.3 1-(5-((4-(4-methoxyphenyl)pyrimidin-2-yl)amino)-1-methyl-1H-indol-3-yl)-2-

(piperidin-1-yl)ethane-1,2-dione (7c): White solid; yield: 61%; mp 239-241 °C; IR (KBr): 3421, 2951, 1625, 1561, 1449, 1409, 1255, 1171, 1032, 798, 736, 583 cm^{-1} ; ^1H NMR (500 MHz, DMSO- d_6) δ 9.64 (1H, s), 9.01 (1H, bs), 8.48 (1H, d, $J = 5.2$ Hz), 8.32 (2H, d, $J = 8.7$ Hz), 8.10 (1H, s), 7.60 (1H, dd, $J = 8.8, 1.8$ Hz), 7.52 (1H, d, $J = 8.8$ Hz), 7.35 (1H, d, $J = 5.2$ Hz), 7.08 (2H, d, $J = 8.8$ Hz), 3.89 (3H, s), 3.85 (3H, s), 3.60 (2H, bs), 3.34 (2H, bs), 1.62 (4H, bs), 1.48 (2H, bs); ^{13}C NMR (125 MHz, DMSO- d_6) δ 185.8, 165.7, 162.9, 161.4, 160.1, 158.6, 139.9, 136.5, 133.0, 128.8, 128.7, 125.5, 116.7, 114.0, 111.8, 110.7, 110.6, 106.5, 55.2, 46.4, 41.1, 33.3, 25.9, 24.9, 23.8; HRMS: m/z calcd for $\text{C}_{27}\text{H}_{27}\text{N}_5\text{O}_3$ $[\text{M}+\text{H}]^+$: 470.2187; found: $[\text{M}+\text{H}]^+$ 470.2182.

4.3.4 1-(5-((4-(4-hydroxyphenyl)pyrimidin-2-yl)amino)-1-methyl-1H-indol-3-yl)-2-

(piperidin-1-yl)ethane-1,2-dione (7d): White solid; yield: 59%; mp 241-244 °C; IR (KBr): 3340, 2937, 1624, 1427, 1212, 1085, 757 cm^{-1} ; ^1H NMR (500 MHz, DMSO- d_6) δ 13.05 (1H, bs), 10.00 (1H, s), 8.58 (1H, d, $J = 5.3$ Hz), 8.41 (1H, s), 8.15 (1H, s), 8.04 (1H, d, $J = 7.9$ Hz), 7.67 (1H, d, $J = 7.3$ Hz), 7.58 (1H, d, $J = 8.8$ Hz), 7.50 (1H, d, $J = 5.4$ Hz), 7.37 (1H, t, $J = 7.6$ Hz), 6.97 – 6.88 (2H, m), 3.90 (3H, s), 3.57 (2H, bs), 3.31 (2H, bs), 1.61 (4H, bs), 1.45 (2H, bs); ^{13}C NMR (125 MHz, DMSO- d_6) δ 185.8, 165.6, 164.1, 159.7, 159.2, 158.3, 140.1, 135.2, 133.9, 132.8, 127.9, 125.5, 118.9, 117.9, 117.3, 111.7, 111.0,

106.2, 46.3, 41.1, 33.3, 25.8, 24.9, 23.8; HRMS: m/z calcd for $C_{26}H_{25}N_5O_3$ $[M+H]^+$: 456.2030; found: $[M+H]^+$ 456.2038.

4.3.5 1-(5-((4-(4-fluorophenyl)pyrimidin-2-yl)amino)-1-methyl-1H-indol-3-yl)-2-

(piperidin-1-yl)ethane-1,2-dione (7e): Yellow solid; yield: 56%; mp 215-218 °C; IR (KBr): 3293, 2937, 1621, 1559, 1416, 1223, 1201, 815, 776 cm^{-1} ; 1H NMR (500 MHz, DMSO- d_6) δ 9.75 (1H, s), 9.05 (1H, bs), 8.55 (1H, d, $J = 5.1$ Hz), 8.48 – 8.39 (2H, m), 8.11 (1H, s), 7.58 (1H, d, $J = 8.8$ Hz), 7.53 (1H, d, $J = 8.8$ Hz), 7.42 (1H, d, $J = 5.2$ Hz), 7.35 (2H, t, $J = 8.7$ Hz), 3.89 (3H, s), 3.59 (2H, bs), 3.33 (2H, bs), 1.62 (4H, bs), 1.47 (2H, bs); ^{13}C NMR (125 MHz, DMSO- d_6) δ 185.9, 165.6, 164.7, 162.7, 160.1, 159.1, 139.9, 136.4, 133.1, 133.0, 129.5, 129.4, 125.5, 116.7, 115.6, 115.5, 111.8, 110.8, 110.6, 107.0, 46.3, 41.1, 33.3, 25.8, 24.9, 23.8 ; HRMS: m/z calcd for $C_{26}H_{24}FN_5O_2$ $[M+H]^+$: 458.1987; found: $[M+H]^+$ 458.1988.

4.3.6 1-(5-((4-(4-chlorophenyl)pyrimidin-2-yl)amino)-1-methyl-1H-indol-3-yl)-2-

(piperidin-1-yl)ethane-1,2-dione (7f): Yellow solid; yield: 62%; mp 211-214 °C; IR (KBr): 3306, 2930, 2854, 1616, 1540, 1442, 1251, 1086, 795, 806, 554 cm^{-1} ; 1H NMR (500 MHz, DMSO- d_6) δ 9.78 (1H, s), 9.07 (1H, bs), 8.58 (1H, d, $J = 5.2$ Hz), 8.40 (2H, d, $J = 8.5$ Hz), 8.12 (1H, s), 7.62 – 7.51 (4H, m), 7.44 (1H, d, $J = 5.2$ Hz), 3.88 (3H, s), 3.60 (2H, bs), 3.34 (2H, bs), 1.63 (4H, bs), 1.48 (2H, bs); ^{13}C NMR (125 MHz, DMSO- d_6) δ 185.9, 165.7, 161.9, 160.1, 159.3, 140.0, 136.3, 135.5, 135.3, 133.1, 128.9, 128.7, 125.5, 116.7, 111.8, 110.8, 110.6, 107.2, 46.3, 41.1, 33.3, 25.8, 24.9, 23.8; HRMS: m/z calcd for $C_{26}H_{24}ClN_5O_2$ $[M+H]^+$: 474.1691; found: $[M+H]^+$ 474.1681.

4.3.7 1-(1-methyl-5-((4-(4-(trifluoromethyl)phenyl)pyrimidin-2-yl)amino)-1H-indol-3-

yl)-2-(piperidin-1-yl)ethane-1,2-dione (7g): Yellow solid; yield: 65%; mp 231-234 °C; IR (KBr): 3302, 2944, 2861, 1620, 1560, 1446, 1325, 1117, 1166, 814, 773 cm^{-1} ; 1H NMR (500 MHz, DMSO- d_6) δ 9.86 (1H, s), 9.10 (1H, bs), 8.63 (1H, d, $J = 5.1$ Hz), 8.58 (2H, d, J

= 7.9 Hz), 8.13 (1H, s), 7.89 (2H, d, $J = 8.3$ Hz), 7.57 (1H, d, $J = 8.9$ Hz), 7.55 – 7.50 (2H, m), 3.89 (3H, s), 3.59 (2H, bs), 3.34 (2H, bs), 1.62 (4H, bs), 1.48 (2H, bs); ^{13}C NMR (125 MHz, DMSO- d_6) δ 185.9, 165.6, 161.6, 160.2, 159.7, 159.5, 140.4, 140.0, 136.2, 133.1, 127.9, 127.8, 125.5, 116.7, 111.8, 110.8, 110.7, 107.7, 46.4, 41.2, 33.3, 25.8, 25.0, 23.8; HRMS: m/z calcd for $\text{C}_{27}\text{H}_{24}\text{F}_3\text{N}_5\text{O}_2$ $[\text{M}+\text{H}]^+$: 508.1955; found: $[\text{M}+\text{H}]^+$ 508.1946.

4.3.8 1-(1-methyl-5-((4-(18ignalli-3-yl)pyrimidin-2-yl)amino)-1H-indol-3-yl)-2-

(piperidin-1-yl)ethane-1,2-dione (**7h**): White solid; yield: 54%; mp 186-189 °C; IR (KBr): 3251, 2927, 1643, 1625, 1553, 1412, 1389, 1196, 1076, 790, 710 cm^{-1} ; ^1H NMR (500 MHz, DMSO- d_6) δ 9.82 (1H, s), 9.41 (1H, d, $J = 1.2$ Hz), 9.23 (1H, d, $J = 1.5$ Hz), 8.96 (1H, bs), 8.68 (1H, dd, $J = 4.7, 1.3$ Hz), 8.61 (1H, d, $J = 5.1$ Hz), 8.39 (1H, d, $J = 8.0$ Hz), 8.36 (1H, d, $J = 5.1$ Hz), 8.12 (1H, s), 7.61 (1H, dd, $J = 8.8, 1.6$ Hz), 7.21 (1H, d, $J = 5.1$ Hz), 3.89 (3H, s), 3.59 (2H, bs), 3.31 (2H, bs), 1.62 (4H, bs), 1.47 (2H, bs); ^{13}C NMR (125 MHz, DMSO- d_6) δ 185.9, 165.6, 161.2, 160.2, 159.3, 151.4, 148.1, 139.9, 136.2, 134.5, 133.2, 132.1, 125.5, 123.8, 116.9, 111.8, 110.9, 110.8, 107.5, 46.4, 41.1, 33.3, 25.8, 24.9, 23.8; HRMS: m/z calcd for $\text{C}_{25}\text{H}_{24}\text{N}_6\text{O}_2$ $[\text{M}+\text{H}]^+$: 441.2034; found: $[\text{M}+\text{H}]^+$ 441.2078.

4.3.9 1-(1-methyl-5-((4-(thiophen-2-yl)pyrimidin-2-yl)amino)-1H-indol-3-yl)-2-

(piperidin-1-yl)ethane-1,2-dione (**7i**): Yellow solid; yield: 52%; mp 214-217 °C; IR (KBr): 3320, 2939, 1618, 1524, 1445, 1207, 1085, 796 cm^{-1} ; ^1H NMR (500 MHz, DMSO- d_6) δ 9.68 (1H, s), 8.69 (1H, bs), 8.47 (1H, d, $J = 5.1$ Hz), 8.10 (1H, s), 8.05 (1H, d, $J = 3.3$ Hz), 7.80 (1H, d, $J = 4.9$ Hz), 7.74 (1H, dd, $J = 8.9, 1.6$ Hz), 7.52 (1H, d, $J = 8.9$ Hz), 7.29 (1H, d, $J = 5.2$ Hz), 7.26 – 7.21 (1H, m), 3.89 (3H, s), 3.58 (2H, bs), 3.31 (2H, bs), 1.62 (4H, bs), 1.46 (2H, bs); ^{13}C NMR (125 MHz, DMSO- d_6) δ 185.7, 165.7, 159.9, 158.6, 142.5, 139.8, 136.2, 133.3, 130.3, 128.5, 128.1, 125.5, 117.0, 111.8, 111.1, 110.6, 105.9, 46.3, 41.1, 33.3, 25.8, 24.9, 23.8; HRMS: m/z calcd for $\text{C}_{24}\text{H}_{23}\text{N}_5\text{O}_2\text{S}$ $[\text{M}+\text{H}]^+$: 446.1645; found: $[\text{M}+\text{H}]^+$ 446.1642.

4.3.10 1-(1-methyl-5-phenyl-1H-indol-3-yl)-2-(piperidin-1-yl)ethane-1,2-dione (8a):

White solid; yield: 74%; mp 154-157 °C; IR (KBr): 2986, 1624, 1525, 1386, 1208, 1008, 949, 759 cm⁻¹; ¹H NMR (500 MHz, CDCl₃) δ 8.60 (1H, s), 7.85 (1H, s), 7.69 (2H, d, *J* = 7.6 Hz), 7.60 (1H, dd, *J* = 8.5, 1.5 Hz), 7.48-7.39 (3H, m), 7.33 (1H, t, *J* = 7.4 Hz), 3.87 (3H, s), 3.69 (2H, bs), 3.47 – 3.44 (2H, m), 1.68 (4H, s), 1.57 – 1.56 (2H, m); ¹³C NMR (125 MHz, CDCl₃) δ 185.7, 166.1, 141.5, 139.4, 137.1, 136.8, 128.6, 127.5, 126.8, 123.6, 120.8, 113.7, 111.3, 110.1, 47.2, 42.3, 33.8, 26.4, 25.5, 24.5; HRMS: *m/z* calcd for C₂₂H₂₂N₂O₂ [M+H]⁺: 347.1754; found: [M+H]⁺ 347.1772.

4.3.11 1-(1-methyl-5-(*p*-tolyl)-1H-indol-3-yl)-2-(piperidin-1-yl)ethane-1,2-dione (8b):

White solid; yield: 72%; mp 159-162 °C; IR (KBr): 3113, 2936, 1731, 1622, 1524, 1264, 1089, 949, 807, 774 cm⁻¹; ¹H NMR (500 MHz, DMSO-*d*₆) δ 8.34 (1H, s), 8.22 (1H, s), 7.67 (1H, d, *J* = 8.5 Hz), 7.62 (1H, dd, *J* = 8.6, 1.7 Hz), 7.57 (2H, d, *J* = 8.1 Hz), 7.29 (2H, d, *J* = 7.9 Hz), 3.93 (3H, s), 3.59 (2H, m), 3.33 – 3.28 (2H, m), 2.35 (3H, s), 1.61 (4H, s), 1.44 (2H, s); ¹³C NMR (125 MHz, DMSO) δ 186.1, 165.5, 140.5, 137.9, 136.9, 136.1, 135.4, 129.5, 126.6, 125.9, 122.6, 118.6, 112.1, 111.5, 46.4, 41.2, 33.4, 25.8, 25.0, 23.8, 20.5; HRMS: *m/z* calcd for C₂₃H₂₅N₂O₂ [M+H]⁺: 361.1911; found: [M+H]⁺ 361.1926.

4.3.12 1-(5-((4-ethylphenyl)amino)-1-methyl-1H-indol-3-yl)-2-(piperidin-1-yl)ethane-

1,2-dione (8c): White solid; yield: 65%; mp 161-164 °C; IR (KBr): 3035, 2954, 1618, 1523, 1363, 1208, 1081, 738 cm⁻¹; ¹H NMR (500 MHz, CDCl₃) δ 8.59 (1H, s), 7.84 (1H, d, *J* = 6.3 Hz), 7.65 – 7.58 (3H, m), 7.42 (1H, dd, *J* = 13.1, 5.2 Hz), 7.29 (2H, d, *J* = 8.0 Hz), 3.87 (3H, s), 3.71 (2H, m), 3.45 (2H, m), 2.71 (2H, q, *J* = 7.6 Hz), 1.69 (4H, m), 1.59 (2H, m), 1.29 (3H, t, *J* = 7.6 Hz); ¹³C NMR (125 MHz, CDCl₃) δ 185.7, 166.1, 142.9, 139.3, 138.8, 136.9, 136.7, 128.1, 127.4, 126.7, 123.5, 120.5, 113.6, 110.8, 47.2, 42.3, 33.8, 28.4, 26.4, 25.5, 24.5, 15.6; HRMS: *m/z* calcd for C₂₄H₂₆N₂O₂ [M+H]⁺: 375.2067; found: [M+H]⁺ 375.2081.

4.3.13 1-(5-(4-chlorophenyl)-1-methyl-1H-indol-3-yl)-2-(piperidin-1-yl)ethane-1,2-dione

(8d): Orange solid; yield: 62%; mp 149-152 °C; IR (KBr): 3133, 2927, 1617, 1528, 1444, 1208, 1087, 948, 848, 764 cm^{-1} ; ^1H NMR (500 MHz, DMSO- d_6) δ 8.45 (2H, d, $J = 1.5$ Hz), 8.29 (1H, s), 8.25 – 8.17 (2H, m), 7.82 – 7.76 (3H, m), 3.96 (3H, s), 3.60 (2H, bs), 3.35 – 3.29 (2H, m), 1.63 (4H, s), 1.46 (2H, s) ^{13}C NMR (125 MHz, DMSO- d_6) δ 186.1, 165.4, 148.3, 142.4, 141.0, 137.6, 133.4, 132.9, 130.5, 125.9, 122.8, 121.6, 121.0, 119.3, 112.2, 112.0, 46.4, 41.2, 33.4, 25.9, 24.9, 23.8; HRMS: m/z calcd for $\text{C}_{22}\text{H}_{21}\text{ClN}_2\text{O}_2$ $[\text{M}+\text{H}]^+$: 381.1364; found: $[\text{M}+\text{H}]^+$: 381.1371.

4.3.14 1-(5-(2,4-dichlorophenyl)-1-methyl-1H-indol-3-yl)-2-(piperidin-1-yl)ethane-1,2-

dione (8e): Yellow solid; yield: 54%; mp 162-165 °C; IR (KBr): 3125, 2991, 1626, 1526, 1444, 1364, 1236, 1085, 949, 775 cm^{-1} ; ^1H NMR (500 MHz, DMSO- d_6) δ 8.25 (1H, s), 8.24 (1H, s), 7.63 (3H, m), 7.55 (1H, m), 7.52 – 7.44 (1H, m), 3.90 (3H, s), 3.58 (2H, bs), 3.30 – 3.25 (2H, m), 1.61 (4H, bs), 1.43 (2H, bs); ^{13}C NMR (125 MHz, DMSO- d_6) δ 186.1, 165.4, 148.3, 142.4, 137.6, 133.4, 132.9, 130.5, 128.8, 125.8, 122.8, 121.6, 121.0, 119.3, 112.1, 112.0, 46.4, 41.2, 33.4, 25.8, 24.9, 23.8 HRMS: m/z calcd for $\text{C}_{22}\text{H}_{20}\text{Cl}_2\text{N}_2\text{O}_2$ $[\text{M}+2\text{H}]^+$: 416.1047; found: $[\text{M}+2\text{H}]^+$: 416.1052.

4.3.15 1-(1-methyl-5-(naphthalen-2-yl)-1H-indol-3-yl)-2-(piperidin-1-yl)ethane-1,2-

dione (8f): Orange solid; yield: 52%; mp 159-162 °C; IR (KBr): 3053, 2856, 1622, 1444, 1363, 1207, 10008, 852, 788 cm^{-1} ; ^1H NMR (500 MHz, CDCl_3) δ 8.56 – 8.47 (1H, m), 7.92-7.88 (1H, m), 7.87-7.84 (1H, m), 7.82(1H, s), 7.69-7.64 (2H, m), 7.58 – 7.38 (5H, m), 7.22 (1H, d, $J = 8.7$ Hz), 3.92 (3H, s), 3.68 (2H, bs), 3.47 – 3.41 (2H, m), 1.72 – 1.64 (4H, m), 1.58 (2H, m); ^{13}C NMR (125 MHz, CDCl_3) δ 185.4, 165.7, 139.5, 136.2, 132.1, 132.0, 128.5, 128.4, 128.1, 127.4, 126.9, 126.3, 126.1, 125.8, 125.5, 125.2, 124.9, 116.9, 111.3, 47.2, 42.4, 33.8, 26.4, 25.5, 24.4; HRMS: m/z calcd for $\text{C}_{26}\text{H}_{24}\text{N}_2\text{O}_2$ $[\text{M}+\text{H}]^+$: 397.1911; found: $[\text{M}+\text{H}]^+$: 397.1918.

4.4 Pharmacology

4.4.1 MTT assay

The anticancer activity of all newly synthesized compounds was determined using MTT assay. $3-5 \times 10^3$ cells per well were seeded in 100 μ L DMEM or RPMI, supplemented with 10% FBS in each well of 96-well microculture plates and incubated for 48 h at 37 °C in a CO₂ incubator. Compounds, diluted to the desired concentrations in culture medium, were added to the wells with respective vehicle control. After 48 h of incubation, drugs containing media was removed and 100 μ L MTT (3-(4,5-dimethylthiazol-2-yl)-2,5-diphenyl tetrazolium bromide) (0.5mg/mL) was added to each well and the plates were further incubated for 4 h. Then, the supernatant from each well was carefully removed, formazon crystals were dissolved in 200 μ L of DMSO and absorbance was recorded at 570 nm wavelength.

4.4.2 Wound healing assay

DU-145 cells (5×10^5 cells/well) were grown in petridishes for 24 h. Scratches were made in confluent monolayers using 200 μ L pipette tip. Then, wounds were washed twice with PBS to remove non-adherent cell debris. The media containing different concentrations (100, 200 and 400 nM) of the compound **7f** were added to the petridishes. Cells which migrated across the wound area were photographed under the phase contrast microscope (Nikon) after 0, 12 and 24 h treatment. The number of cells migrated in to the wound area was counted manually.

4.4.3 Acridine orange–ethidium bromide (AO–EB) staining

DU145 cells were plated at a concentration of 1×10^6 cell/ml and treated with different concentration of compound **7f**. Plates were incubated in an atmosphere of 5% CO₂ at 37 °C for 48 h. 10 μ L of fluorescent dyes containing Acridine Orange (AO) and Ethidium Bromide

(EB) added into each well in equal volumes (10 $\mu\text{g}/\text{mL}$) respectively and within 10 min the cells were visualized under fluorescence microscope (Nikon, Inc. Japan) with excitation (488 nm) and emission (550 nm) at 200x magnification.

4.4.4 DAPI Nucleic Acid Staining

Nuclear morphological changes were observed through DAPI staining. After treatment with **7f** for 48 h in DU145 cells, cells were washed with PBS and permeabilized with 0.1 % Tween 20 for 10 min followed by staining with 1 μM DAPI. Control and Treated cells were observed with fluorescence microscope (Model: Nikon, Japan) with excitation at 359 nm and emission at 461 nm using DAPI filter at 200X magnification.

4.4.5 Cell cycle analysis

Flow cytometric analysis (FACS) was performed to calculate the distribution of the cell population through the cell cycle phases. DU145 cancer cells were incubated with compound **7f** at varied concentration of 200 and 400 nM for 24 h. Untreated and treated cells were harvested, washed with PBS, fixed in ice-cold 70% ethanol and stained with propidium iodide (50 $\mu\text{g}/\text{mL}$, sigma 22ignall) in the presence of Rnase A (20 $\mu\text{g}/\text{mL}$) containing 0.1% Triton X-100 for 30 min at 37 °C in dark, and about 10000 events were analyzed by flow cytometer (BD FACSVerserTM, USA).

4.4.6 Annexin V binding assay

DU145 cells (1×10^6) were seeded in six-well plates and allowed to grow overnight. The medium was then replaced with complete medium containing compound **7f** at 200, 400 nM concentrations and 400 nM concentration of indibulin. After 24 h of treatment, cells from the supernatant and adherent monolayer cells were harvested by trypsinization, washed with PBS at 3000 rpm. Then the cells were processed with Annexin V-assay kit (FITC Annexin V

Apoptosis Detection Kit, BD Pharmingen™) according to the manufacturer's instruction. Further, flow cytometric analysis was performed using a flow cytometer (BD FACSVerser™, USA).

4.4.7 Measurement of Mitochondrial Membrane Potential

DU145 cells (1×10^6 cells/mL) were seeded in 6 well plates and allowed to adhere for overnight. The cells were incubated with 200, 400 nM concentrations of the compound **7f** and 400 nM concentration of podophyllotoxin for 24 h. Cells were collected, washed with PBS and resuspended in solution of JC-1 (2.5 μ g/mL) and incubated for 45 min in incubator at 37 °C. The cells were washed twice with PBS and cells were trypsinized, centrifuged and analysed by flow cytometer (BD FACSVerser™, USA).

4.4.8 Measurement of Superoxide levels

Mitochondrial superoxide ($O_2^{\cdot-}$) generation was determined by using MitoSOX™ Red dye. In this assay, DU-145 cells were seeded at a density of 5×10^5 cells/mL in a 24-well plate and allowed to adhere overnight. Cells were treated with increasing concentrations of **7f** (100, 200 and 400 nM) for 48 h. After the treatment, cells were incubated with a solution of MitoSOX™ Red mitochondrial superoxide indicator (5 μ M) in HBSS (Hank's balanced salt solution) for 15 min at 37 °C. Cells were then washed three times with PBS to remove the excess dye. Images were captured using the fluorescent microscope (BIORAD).

4.4.9 *In vitro* tubulin polymerization

A fluorescence based *in vitro* tubulin polymerization assay was performed according to the manufacturer's protocol (BK011, Cytoskeleton, Inc.). Briefly, the reaction mixture in a total volume of 10 μ L contained PEM buffer, GTP (1 μ M) in the presence or absence of test compounds **7f** (0.5 μ M), indibulin (0.5 μ M), podophyllotoxin (5 μ M). Tubulin

polymerization was followed by a time dependent increase in fluorescence due to the incorporation of a fluorescence reporter into microtubules as polymerization proceeds. Fluorescence emission at 420 nm (excitation wavelength is 360 nm) was measured by using a Varioscan multimode plate reader (Thermo scientific Inc.). The IC₅₀ value was defined as the drug concentration required to inhibit 50% of tubulin assembly compared to control. The reaction mixture for these experiments include: tubulin (3 mg/mL) in PEM buffer, GTP (1 mM), in the presence or absence of test compounds at various concentrations. Polymerization was monitored by increase in the fluorescence as mentioned above at 37 °C.

4.4.10 Western blotting analysis

Primary antibodies against Bax, Bcl-2, PARP, Cyt c, β -actin and HRP conjugated antirabbit secondary antibodies were purchased from Cell Signaling Technology (Danvers, MA, USA). Equal amounts of protein sample (25 μ g/lane) from each experimental group and were separated by SDS–polyacrylamide gel electrophoresis. Then the protein bands were transferred to polyvinylidene fluoride membrane (Pierce Biotechnology, Rockford, IL, USA) for western blotting. Membranes were blocked with 3% bovine serum albumin in TBS buffer (pH-7.4) and incubated with the indicated antibodies overnight at 4 °C. β -actin (1:1000) was used for equal loading. After washing the membranes in TBST buffer, membranes were exposed to the HRP-conjugated secondary antibodies (1:5000) for 2 h at room temperature. The reactive bands were visualized with chemiluminescent detection reagents (Supersignal West Pico, Pierce Biotechnology, Rockford, IL, USA). The densitometry analysis of the blots was performed by using Image J software, NIH, USA.

Acknowledgements

Authors are thankful to DoP, Ministry of Chemicals & Fertilizers, Govt. Of India, New Delhi, for the award of NIPER fellowship.

References

1. K.C. Nicolaou, F. Roschangar, D. Vourloumis, Chemical biology of epothilones, *Angew. Chem. Int. Ed.* 37 (1998) 2014–2045.
2. R. Kaur, P. Kaur, S. Sharma, G. Singh, S. Mehndiratta, K. Nepali, Anti-cancer pyrimidines in diverse scaffolds: A review of patent literature, *Recent Pat. Anti Cancer Drug Discov.* 10 (2015) 23–71.
3. S. Sharma, S. Mehndiratta, S. Kumar, J. Singh, P.M.S. Bedi, K. Nepali, Purine analogues as kinase inhibitors: a review, *Recent Pat. Anti Cancer Drug Discov.* 10 (2015) 308–341.
4. A. Brancale, R. Silvestri, Indole, a core nucleus for potent inhibitors of tubulin polymerization, *Med. Res. Rev.* 27 (2007), 209–238.
5. J. J. Field, A. Kanakkanthara, J. H. Miller, Microtubule-targeting agents are clinically successful due to both mitotic and interphase impairment of microtubule function, *Bioorg. Med. Chem.* (22) 2014 5050–5059.
6. S. Sharma, C. Kaur, A. Budhiraja, K. Nepali, M.K. Gupta, A.K. Saxena, P.M.S. Bedi, Chalcone based azacarboline analogues as novel antitubulin agents: Design, synthesis, biological evaluation and molecular modelling studies, *Eur. J. Med. Chem.* 85 (2014) 648–660.
7. M. A. Jordan, L. Wilson, Microtubules as a target for anticancer drugs, *Nat. Rev. Cancer.* 4 (2004) 253–265.

8. M. Alami, S. Messaoudi, B. Treguier, A. Hamze, O. Provot, J. F. Peyrat, J. R. De Losada, J. M. Liu, J. Bignon, J. Wdzieczak-Bakala, S. Thoret, J. Dubois, J. D. Brion, Iso combretastatins A versus combretastatins A: The forgotten iso CA-4 isomer as a highly promising cytotoxic and antitubulin agent, *J. Med. Chem.* 52 (2009) 4538–4542.
9. G. Bacher, B. Nickel, P. Emig, U. Vanhoefer, S. Seeber, A. Shandra, T. Klenner, T. Beckers, D-24851, a novel synthetic microtubule inhibitor, exerts curative antitumoral activity in vivo, shows efficacy toward multidrug-resistant tumor cells, and lacks neurotoxicity, *Cancer Res.* 61 (2001), 392–399.
10. P. Marchand, M. Antoine, G. Le Baut, M. Czech, S. Baasner, E. Günther, Synthesis and structure–activity relationships of N-aryl (indol-3-yl) glyoxamides as antitumor agents, *Bioorg Med Chem Lett.* 17 (2009) 6715–6727.
11. (a) X. Zhang, S. Raghavan, M. Ihnat, J.E. Thorpe, B.C. Disch, A. Bastian, L.C. Bailey-Downs, N.F. Dybdal-Hargreaves, C.C. Rohena, E. Hamel, S.L. Mooberry, A. Gangjee, The design and discovery of water soluble 4-substituted-2, 6-dimethylfuro [2, 3-d] pyrimidines as multitargeted receptor tyrosine kinase inhibitors and microtubule targeting antitumor agents, *Bioorg Med Chem.* 22 (2014) 3753–3772; (b) X. Zhang, S. Raghavan, M. Ihnat, E. Hamel, C. Zammiello, A. Bastian, S.L. Mooberry, A. Gangjee, The design, synthesis and biological evaluation of conformationally restricted 4-substituted-2, 6-dimethylfuro [2, 3-d] pyrimidines as multi-targeted receptor tyrosine kinase and microtubule inhibitors as potential antitumor agents, *Bioorg Med Chem.* 23 (2015) 2408–2423.
12. F. Xie, H. Zhao, L. Zhao, L. Lou, Y. Hu, The design, synthesis and biological evaluation of conformationally restricted 4-substituted-2, 6-dimethylfuro [2, 3-d]

- pyrimidines as multi-targeted receptor tyrosine kinase and microtubule inhibitors as potential antitumor agents, *Bioorg Med Chem Lett.* 19 (2009) 275–278.
13. F. Xie, H. Zhao, D. Li, H. Chen, H. Quan, X. Shi, L. Lou, Y. Hu, Synthesis and biological evaluation of 2, 4, 5-substituted pyrimidines as a new class of tubulin polymerization inhibitors, *J Med Chem.* 54 (2011) 3200–3205.
14. N. K. Kaushik, N. Kaushik, P. Attri, N. Kumar, C. H. Kim, A. K. Verma, E. H. Choi, Biomedical importance of indoles, *Molecules.* 18 (2013) 6620–6662.
15. C.-J. Chang, R. L. Geahlen, Protein-tyrosine kinase inhibition: mechanism-based discovery of antitumor agents, *J. Nat. Prod.* 55 (1992) 1529–1560.
16. S. B. Bharate, S. D. Sawant, P. P. Singh, R. A. Vishwakarma, Kinase inhibitors of marine origin, *Chem. Rev.* 113 (2013) 6761–6815.
17. G. M. Cragg, P. G. Grothaus, D. J. Newman, Impact of Natural products on developing new anti-cancer agents, *Chem. Rev.* 109 (2009) 3012–3043.
18. (a) A. Nagarsenkar, L. Guntuku, S. D. Guggilapu, K. Dantibai, S. Gannoju, V. G. M. Naidu, B. N. Babu, Synthesis and apoptosis inducing studies of triazole linked 3-benzylidene isatin derivatives, *Eur. J. Med. Chem.* 124 (2016) 782–793; (b) A. Nagarsenkar, S. K. Prajapati, S. D. Guggilapu, S. Birineni, S. S. Kotapalli, R. Ummanni, B. N. Babu, Investigation of triazole-linked indole and oxindole glycoconjugates as potential anticancer agents: novel Akt/PKB 27 signalling pathway inhibitors, *Med. Chem. Commun.* 7 (2016) 646–653; (c) S. K. Prajapati, A. Nagarsenkar, S. D. Guggilapu, K. K. Gupta, L. Allakonda, M. K. Jeengar, V. G. M. Naidu, B. N. Babu, Synthesis and biological evaluation of oxindole linked indolyl-pyrimidine derivatives as potential cytotoxic agents, *Bioorg. Med. Chem. Lett.* 26 (2016) 3024–3028; (d) S. D. Guggilapu, S. K. Prajapati, A. Nagarsenkar, G. Lalita, V. G. M. Naidu, B. N. Babu, MoO₂ Cl₂ catalyzed efficient synthesis of functionalized 3,

- 4-dihydropyrimidin-2 (1*H*)-ones/thiones and polyhydroquinolines: recyclability, fluorescence and biological studies, *New J. Chem.* 40 (2016) 838–843.
19. P. F. Schuda, C. B. Ebner, T. M. Morgan, The synthesis of mannich bases from ketones and esters via enaminones, *Tetrahedron Lett.* 27 (1986) 2567–2570.
20. J. Sperry, A concise synthesis of meridianin F, *Tetrahedron Lett.* 52 (2011) 4537–4538.
21. W.-T. Li, D.-R. Hwang, C.-P. Chen, C.-W. Shen, C.-L. Huang, T.-W. Chen, C.-H. Lin, Y.-L. Chang, Y.-Y. Chang, Y.-K. Lo, H.-Y. Tseng, C.-C. Lin, J.-S. Song, H.-C. Chen, S.-J. Chen, S.-H. Wu, C.-T. Chen, Synthesis and biological evaluation of *N*-heterocyclic indolyl glyoxylamides as orally active anticancer agents, *J. Med. Chem.* 46 (2003) 1706–1715.
22. Y. Liu, Y. Bai, J. Zhang, Y. Li, J. Jiao and X. Qi, Optimization of the Conditions for Copper-Mediated *N*-Arylation of Heteroarylamines, *Eur. J. Org. Chem.* (2007) 6084–6088.
23. M. L. Go, J. L. Leow, S. K. Gorla, A. P. Schuller, M. Wang, P.J. Casey, Amino derivatives of indole as potent inhibitors of isoprenylcysteine carboxyl methyltransferase, *J. Med. Chem.* 53 (2010) 6838–6850.
24. S. Shrivastava, P. Kulkarni, D. Thummuri, M. K. Jeengar, V. G. M. Naidu, M. Alvala, G. B. Reddy, S. Ramakrishna, Piperlongumine, an alkaloid causes inhibition of PI3 K/Akt/mTOR 28 signalling axis to induce caspase-dependent apoptosis in human triple-negative breast cancer cells, *Apoptosis.* 19 (2014) 1148–1164.
25. L. G. Rodriguez, X. Wu, J. L. Guan, Wound-healing assay, *Methods Mol. Biol.* 294 (2005) 23–29.

26. U. V. Mallavadhani, N. R. Vanga, M. K. Jeengar, V. G. M. Naidu, Synthesis of novel ring-A fused hybrids of oleanolic acid with capabilities to arrest cell cycle and induce apoptosis in breast cancer cells, *Eur. J. Med. Chem.* 74 (2014) 398–404.
27. S. G. Kennedy, E. S. Kandel, T. K. Cross, N. Hay, Akt/Protein kinase B inhibits cell death by preventing the release of cytochrome c from mitochondria, *Mol. Cell Biol.* 19 (1999) 5800–5810.
28. T. S. Reddy, H. Kulhari, V. G. Reddy, V. Bansal, A. Kamal, R. Shukla, Design, synthesis and biological evaluation of 1, 3-diphenyl-1*H*-pyrazole derivatives containing benzimidazole skeleton as potential anticancer and apoptosis inducing agents, *Eur. J. Med. Chem.* 101 (2015) 790–805.
29. L. J. Browne, C. Gude, H. Rodriguez, R. E. Steele, A. Bhatnager, Fadrozole hydrochloride: a potent, selective, nonsteroidal inhibitor of aromatase for the treatment of estrogen-dependent disease, *J. Med. Chem.* 34 (1991) 725–736.
30. T.S. Reddy, H. Kulhari, V.G. Reddy, A.V.S. Rao, V. Bansal, A. Kamal, R. Shukla, Synthesis and biological evaluation of pyrazolo–triazole hybrids as cytotoxic and apoptosis inducing agents, *Org. Biomol. Chem.* 13 (2015) 10136–10149.
31. E. –R. Hahm, M. B. Moura, E. E. Kelley, B. V. Houten, S. Shiva, S. V. Singh, Withaferin A-induced apoptosis in human breast cancer cells is mediated by reactive oxygen species, *Plos One.* 6 (2011) e23354.
32. V. P. Vineetha, S. Girija, R. S. Soumya, K. G. Raghu, Polyphenol-rich apple (*Malus domestica* L.) peel extract attenuates arsenic trioxide induced cardiotoxicity in H9c2 cells via its antioxidant activity, *Food Funct.* 5 (2014) 502–511.
33. C. Kanthou, O. Greco, A. Stratford, I. Cook, R. Knight, O. Benzakour, G. Tozer, The tubulin-binding agent combretastatin A-4-phosphate arrests endothelial cells in mitosis and induces mitotic cell death, *Am. J. Pathol.* 165 (2004) 1401–1411.

34. K. Huber, P. Patel, L. Zhang, H. Evans, A. D. Westwell, P. M. Fischer, S. Chan, S. Martin, 2-[(1-methylpropyl) dithio]-1H-imidazole inhibits tubulin polymerization through cysteine oxidation, *Mol. Cancer Ther.* 7 (2008) 143–151.
35. Hideakiito, T. Kanzawa, S. Kondo, Y. Kondo, Microtubule inhibitor D-24851 induces p53-independent apoptotic cell death in malignant glioma cells through Bcl-2 phosphorylation and Bax translocation, *Int. J. Oncol.* 26 (2005) 589–596.
36. M. C. Wei, W. -X. Zong, E. H. Y. Cheng, T. Lindsten, V. Panoutsakopoulou, A. J. Ross, K. A. Roth, G. R. MacGregor, C. B. Thompson, S. J. Korsmeyer, Proapoptotic BAX and BAK: a requisite gateway to mitochondrial dysfunction and death, *Science.* 292 (2001) 727–730.

Figures captions, Tables, Figures and Schemes

Figure 1. Structure of some representative bioactive compounds containing indole and pyrimidine moieties.

Figure 2. Design of C₅ tethered indolyl-3-glyoxylamide derivatives as anti-cancer agents.

Figure 3. Effect of compound **7f** on *in vitro* migration potential of DU145 prostate cancer cells. Scratches were created with sterile 200 μ L pipette and images were captured using phase contrast microscopy at 0 h, 12h and 24 h after treatment with 100 nM, 200 nM and 400 nM of compound **7f**.

Figure 4. AO/EB staining of compound **7f** in DU145 cells. Apoptotic features such as membrane blebbing, condensed nuclei and apoptotic body formations were clearly observed in cells treated with indicated conc. Of **7f** in conc. Dependent manner.

Figure 5. Assessment of nuclear morphological changes by DAPI staining in DU145 cells after 48 h. **7f** treated DU145 cells have displayed nuclear apoptotic characteristics such as nuclear fragmentation and shrunken nuclei.

Figure 6. Effect of compound **7f** on cell cycle progression of DU145 cells. The analysis of cell cycle distribution was performed by using propidium iodide staining method. Data represent one of three independent experiments.

Figure 7. Flow cytometry analysis of apoptotic cells after Annexin V-FITC/propidium iodide (PI) staining (representative result of three independent experiments).

Figure 8. Effect of compound **7f** on mitochondrial membrane potential ($D\Psi m$). DU145 cells were treated with different concentrations (200, 400 nM respectively) of compound **7f**, 400nM of podophyllotoxin incubated with JC-1 and analysed by flow cytometer (BD FACSVerserTM, USA).

Figure 9. Effect of compound **7f** on production of superoxide in DU145 cancer cells. Fluorescent microscopic images of DU145 cells stained with MitoSOX after 48 h of treatment with different concentrations of compound **7f**.

Figure 10. Effect of compound **7f** on the tubulin polymerization: tubulin polymerization was monitored by the increase in fluorescence at 360 nm (excitation) and 420 nm (emission) for 1 h at 37 °C.

Figure 11. Effect of **7f** on various protein expressions in DU145 cell line: Results were expressed as mean \pm SEM (n=3). NC: Normal control, 200 and 400 nM **7f** indicate cells treated with 200 & 400 nM of **7f** and 400 nM indibulin indicate cells treated with 400 nM of indibulin for 48 hrs. *P < 0.05, **P < 0.01, ***P < 0.001 Vs NC. Statistical analyses were performed using one-way analysis of variance, followed by the two-tailed Student's t-test.

Table 1. *In vitro* anticancer activity of compounds **7a-7i** and **8a-8f**.

Compound	IC ₅₀ (μM)			
	DU145	PC-3	A549	HCT-15
7a	>50	>50	>50	>50
7b	34.3±3.2	>50	>50	>50
7c	29.3±2.78	36.56±0.63	39.7±2.8	0.42±0.7
7d	>50	>50	>50	>50
7e	0.18±1.25	2.8±1.21	1.6±2.3	3.2±1.5
7f	0.14±0.01	0.22±0.03	1.2±0.1	0.26±0.03
7g	5.91±0.2	>50	14.4±2.6	>50
7h	5.8±0.08	13.20±0.26	1.8±0.64	>50
7i	10.1±0.11	31.2±1.1	>50	>50
8a	>50	>50	>50	>50
8b	32.57±0.9	>50	>50	9.6±1.5
8c	22.13±1.2	>50	>50	>50
8d	>50	>50	>50	>50
8e	>50	>50	>50	>50
8f	>50	>50	>50	>50
Indibulin	0.18±0.03	0.40±0.01	2.1±0.23	0.56±0.05
Podophyllotoxin	0.063±0.008	0.07±0.003	0.09±0.009	0.061±0.005

Table 2: Antitubulin activity of compound **7f**

Compound	IC ₅₀ ^a (μM)
7f	0.40±0.02
Indibulin	0.43±0.02
Podophyllotoxin	0.35±0.06

^aHalf maximal inhibitory concentration: compound concentration required to inhibit tubulin polymerization by 50%; data are the mean ± SD of n=3 independent experiments performed in triplicate.

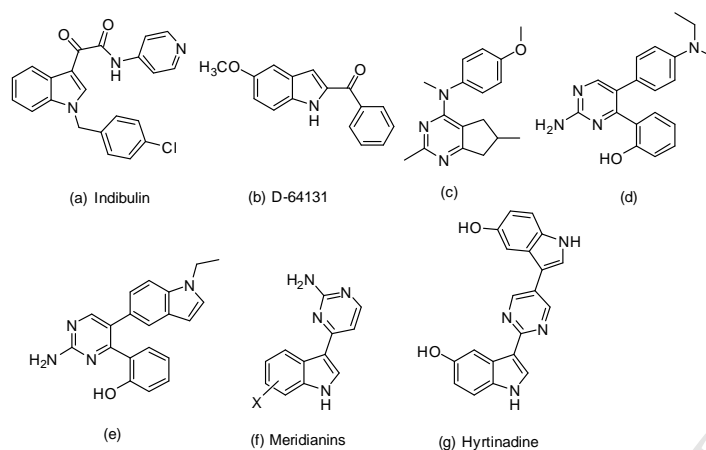


Figure 1. Structure of some representative bioactive compounds containing indole and pyrimidine moieties.

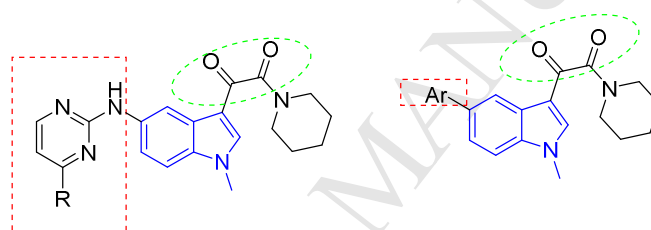


Figure 2. Design of C_5 -tethered indolyl-3-glyoxylamide derivatives as anti-cancer agents.

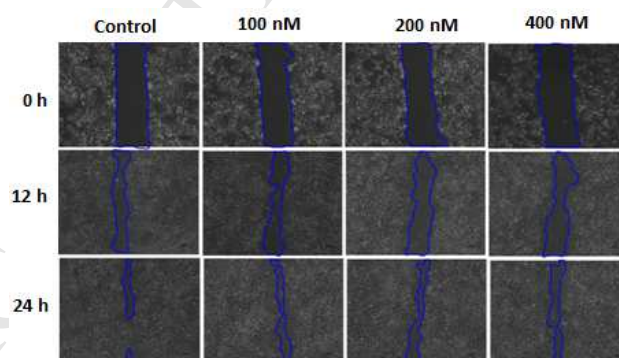


Figure 3. Effect of compound **7f** on *in vitro* migration potential of DU145 prostate cancer cells. Scratches were created with sterile 200 μ L pipette and images were captured using phase contrast microscopy at 0 h, 12h and 24 h after treatment with 100 nM, 200 nM and 400 nM of compound **7f**.

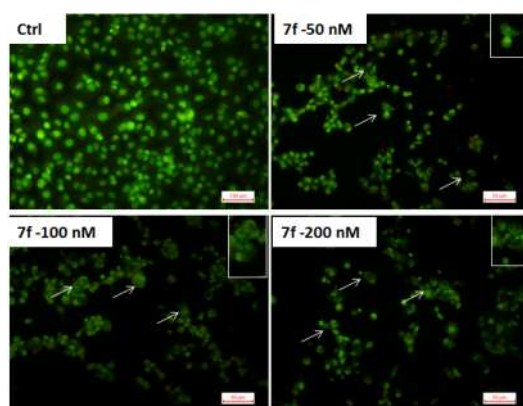


Figure 4. AO/EB staining of compound **7f** in DU145 cells. Apoptotic features such as membrane blebbing, condensed nuclei and apoptotic body formations were clearly observed in cells treated with indicated conc. of **7f** in conc. dependent manner.

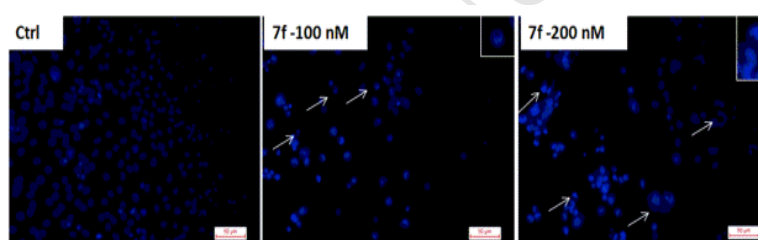


Figure 5. Assessment of nuclear morphological changes by DAPI staining in DU145 cells after 48 h. **7f** treated DU145 cells have displayed nuclear apoptotic characteristics such as nuclear fragmentation and shrunken nuclei.

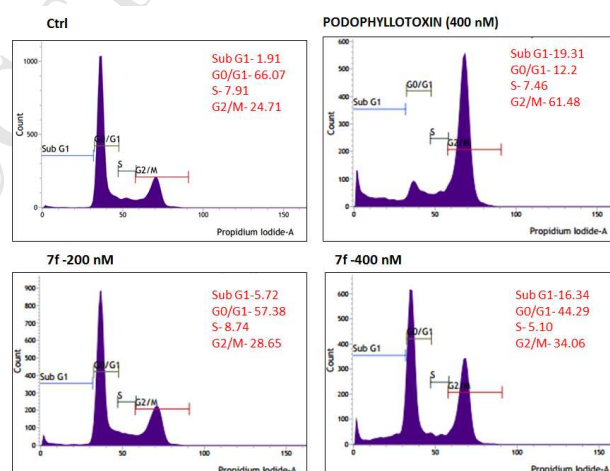


Figure 6. Effect of compound **7f** on cell cycle progression of DU145 cells. The analysis of cell cycle distribution was performed by using propidium iodide staining method. Data represent one of three independent experiments.

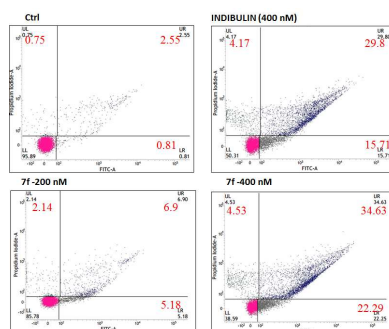


Figure 7. Flow cytometry analysis of apoptotic cells after Annexin V-FITC/propidium iodide (PI) staining (representative result of three independent experiments).

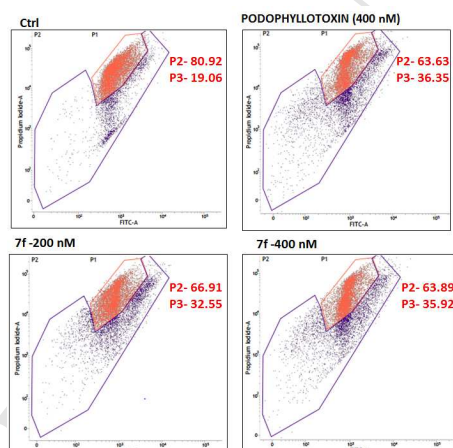


Figure 8. Effect of compound **7f** on mitochondrial membrane potential ($\Delta\Psi_m$). DU145 cells were treated with different concentrations (200, 400 nM respectively) of compound **7f**, 400nM of podophyllotoxin incubated with JC-1 and analysed by flow cytometer (BD FACSVerserTM, USA).

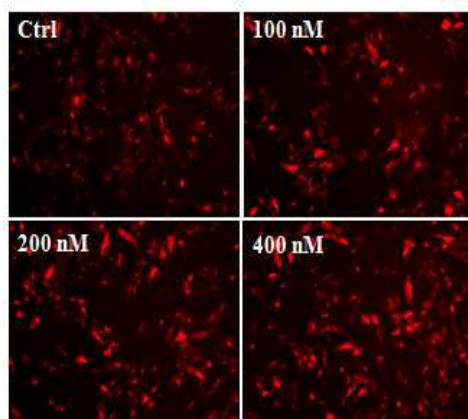


Figure 9. Effect of compound **7f** on production of superoxide in DU145 cancer cells. Fluorescent microscopic images of DU145 cells stained with MitoSOX after 48 h of treatment with different concentrations of compound **7f**.

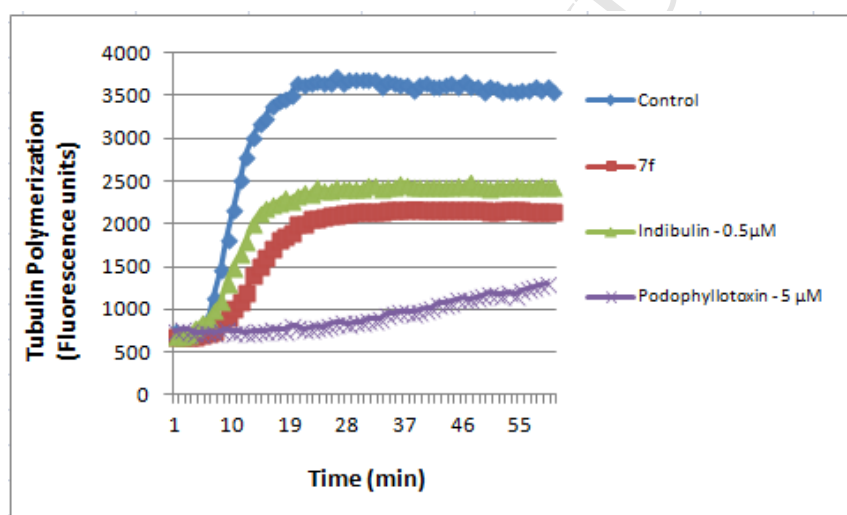


Figure 10. Effect of compound **7f** on the tubulin polymerization: tubulin polymerization was monitored by the increase in fluorescence at 360 nm (excitation) and 420 nm (emission) for 1 h at 37 °C.

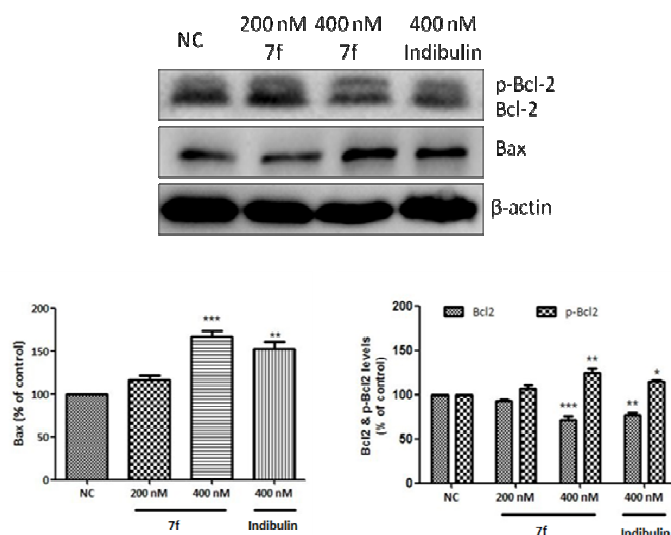
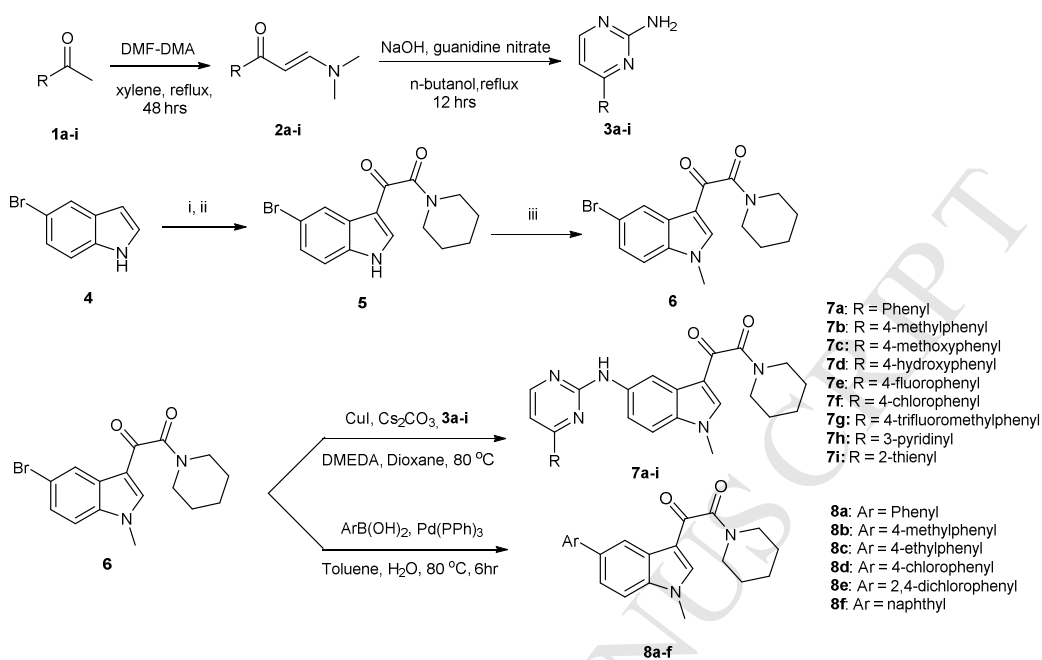


Figure 11. Effect of **7f** on various protein expressions in DU145 cell line: Results were expressed as mean \pm SEM (n=3). NC: Normal control, 200 and 400 nM **7f** indicate cells treated with 200 & 400 nM of **7f** and 400 nM indibulin indicate cells treated with 400 nM of indibulin for 48 hrs. *P < 0.05, **P < 0.01, ***P < 0.001 Vs NC. Statistical analyses were performed using one-way analysis of variance, followed by the two-tailed Student's t-test.



Scheme 1. Synthesis of C₅-tethered indolyl-3-glyoxylamide derivatives; Reagents and conditions: i) oxalyl chloride, diethyl ether, 0 °C; ii) piperidine, triethylamine, tetrahydrofuran, 0 °C; iii) methyl iodide, K₂CO₃, acetonitrile, 60 °C, 4h.

RESEARCH HIGHLIGHTS

- C₅ substituted indolyl-3-glyoxylamides were synthesized.
- Anticancer evaluation of the compounds on selected human cancer cell lines.
- **7f** induced apoptosis and G2/M cell cycle arrest.
- **7f** led to up-regulation of Bax and down-regulation of Bcl-2 apoptotic proteins.